

# The flow-based market coupling domain - Why we can't get it right

Björn Felten, Paul Osinski<sup>\*</sup>, Tim Felling, Christoph Weber

Chair for Management Science and Energy Economics, University of Duisburg-Essen, Germany

## ARTICLE INFO

### JEL classification:

C61  
C80  
D61  
Q41  
Q43  
Q48

### Keywords:

Flow-based market coupling  
Zonal pricing  
Welfare

## ABSTRACT

Significant welfare gains can be achieved by interlinking electric power systems. A major improvement in this regard has been the implementation of flow-based market coupling (FBMC) in Central Western Europe [Réseau de transport d'électricité (RTE) et al., 2015]. However, recent assessments [Entso-E, 2018] have shown that FBMC is not yet fully understood. We contrast the FBMC domain with the feasible regions in a nodal market design based on a stylized example. Our analysis reveals the essential elements of FBMC, including its positive features. We also show that certain FBMC approximations will always affect welfare to a certain extent.

## 1. Introduction

The design of electricity markets has been subject to vigorous debates over the last three decades. One feature of electricity markets is the existence of relevant grid constraints. In conjunction with the very limited storage possibilities for electricity, this makes congestion management a key issue in electricity market design. The European system has been moving towards an improved congestion management, e.g., by introducing implicit market coupling. The last substantial move in that direction has been the introduction of flow-based market coupling (FBMC<sup>1</sup>) for the electricity markets in Central West Europe (CWE, i.e., France, Belgium, Luxembourg, the Netherlands and Germany) in May 2015.

We analyze the FBMC domain or, in more technical terms, the feasible region of the market clearing algorithm under FBMC. We present a stylized example which serves for identifying the effect of all essential elements of the FBMC capacity allocation process (see list below). At the same time, the example is suitable to monitor the actual physical constraints of the grid. As these physical constraints are considered in nodal market designs, our stylized analysis can be seen as a zonal-vs.-nodal assessment. Such studies are not new. Existing studies usually solve the electricity market clearing problems under both market designs (zonal and nodal). For example, by assessing resulting differences in welfare, the effectiveness of the market designs can then be

compared. In the assessments of the nodal market designs, the consideration of load-flow constraints of transmission lines is quite similar in all studies, as it constitutes the straightforward translation of physical properties of the grid. This is not the case for zonal market designs, and existing studies differ in this regard. Based on how load flow constraints are considered in zonal market designs, two groups of studies may be distinguished:

1. **Nodal knowledge:** Load flows are calculated based on information on power injections/withdrawals at the nodal level and using individual line sensitivities. Thus, the state of the power system is known and considered at the highest possible spatial granularity. How market clearing considers zone delimitations can vary. In some cases, explicit price equality constraints within zones are added to the clearing problem (e.g., in [Bjørndal and Jörnsten 2001; Ehrenmann and Smeers 2005; Bjørndal and Jörnsten 2007; Androcec and Krajcar 2012]). In other cases, intra-zonal load flow constraints are excluded from the clearing problem (e.g., in [Bjørndal et al., 2003; Grimm et al., 2016a, b]). In latter cases, the limit values for load flows on inter-zonal lines may be downsized to prevent intra-zonal congestion (cf. [Bjørndal et al., 2003]).
2. **Aggregated grid:** Load flows or exchanges across borders are aggregated (cf. [Ehrenmann and Smeers 2005; Oggioni and Smeers 2012; Oggioni and Smeers 2013; Neuhoff et al., 2013; Grimm et al.,

<sup>\*</sup> Corresponding author.

E-mail address: [paul.osinski@uni-due.de](mailto:paul.osinski@uni-due.de) (P. Osinski).

<sup>1</sup> A list of abbreviations and symbols is given in appendix B.

2016a]). For approximating load flows and line constraints, aggregated grid models are used, which only consider demand and supply balances at the zonal level, i.e., at a much lower spatial resolution than the market clearing mechanisms under numeral 1. The limit values for these flows are sometimes determined by summing up line capacities or by other operations (cf. [Ehrenmann and Smeers 2005]). Frequently, constraints of the EMCP are not imposed on aggregated physical values (i.e., load flows) but on commercial transactions (i.e., bilateral exchanges, cf. [Oggioni and Smeers 2012; Oggioni and Smeers 2013; Neuhoff et al., 2013; Grimm et al., 2016a]). This particular case of constraint formulation implies that only “sensitivity” factors of zeros and ones are used. The latter design corresponds to ATC-based market clearing (cf. [Van den Bergh et al., 2016]).

All of these studies have contributed to the discourse on zonal market designs. For example [Bjørndal and Jörnsten 2001], and [Ehrenmann and Smeers 2005] reveal significant shortcomings, notably welfare losses, of several zonal market designs. Notably, the studies that consider aggregated grids are closest to the analyses presented in this paper. The similarity can especially be seen when considering zonal demand and supply balances, as is the case in FBMC. However, since the publication of these papers, the transmission system operators (TSOs) in CWE, regulatory authorities and other involved parties have made considerable efforts setting up the FBMC methodology and elaborating its procedures [Réseau de transport d’électricité (RTE) et al., 2015]. Most of these new developments are not considered in the prior research. For example, some of these relevant design choices that have been made for FBMC are the following: The consideration of individual lines (i.e., no aggregated grid representation) which also includes selected intra-zonal lines, the use of so-called generation shift keys (GSKs), the consideration of a base case, the use of flow reliability margins (FRMs) and the non-consideration of bids and asks at nodal level (i.e., no nodal knowledge). Due to these elaborate procedures, certain improvements compared to the early concepts of market coupling can be expected and revisiting the zonal market design with focus on the essential FBMC concepts seems expedient. There is an evident need for such analysis, as the European Network of Transmission System Operators (Entso-E) has encountered “non-resolvable complexities” in the course of its Bidding Zone Study [Entso-E, 2018]. To a great extent, the complexities mentioned by Entso-E refer to “essential market design features (especially regarding the design of the capacity calculation approach, e.g. base case approach, CBCO selection, GSK strategy)”. To the best of our knowledge, there is no zonal-vs.-nodal assessment which analyzes these essential FBMC design choices. In turn, the paper at hand presents a novel approach of analyzing all these features of FBMC. We have found a transparent and reproducible example which allows us to give a full description of the feasible region of the zonal market clearing problem and contrasting it with subspaces of the nodal feasible region. Both the consideration of essential FBMC concepts in zonal-vs.-nodal analyses and the distinct illustration provide a sound basis to compare the economic optimum achievable in zonal and nodal markets. These aspects make our analyses novel and unique.

There is a body of literature on FBMC. Apart from Entso-E procedures, descriptive papers on FBMC exist [Plancke et al., 2016; Van den Bergh et al., 2016]. Such descriptions are sometimes extended by statistical assessments [Jegleim 2015; Morin 2016; Kristiansen 2020]. Recently, some model-based assessments of FBMC have been developed [Finck et al., 2018; Marjanovic et al., 2018; Sebestyén et al., 2018; Wyrwoll et al., 2018; Wyrwoll et al., 2019; Matthes et al., 2019; Lang et al., 2020; Schönheit et al., 2020]. Some of these assessments deal with a comparison of ATC-based market coupling and FBMC in Central Eastern Europe [Marjanovic et al., 2018; Finck et al., 2018; Lang et al., 2020], others analyze the impact of FBMC procedures on exchange flows/trading volumes [Wyrwoll et al., 2018; Wyrwoll et al., 2019; Schönheit et al., 2020] or market clearing results [Sebestyén et al., 2018;

Matthes et al., 2019].

However, the paper at hand uses a fundamentally different approach. Instead of performing specific sensitivity analyses, it seeks for more general conclusions on the FBMC design. Using novel analyses of the FBMC domain allows us to scrutinize the cause and effect relations of FBMC procedures. Eventually, we can analyze the benefits and shortcomings of all relevant FBMC mechanisms and parameters. Thereby we show where FBMC can be enhanced and how its potential for improvement is limited due to general market design choices.

A second distinction of this research is its focus on the welfare resulting from the entire FBMC process. We consider not only day-ahead and intraday market clearing, but also redispatch amounts and costs. It explains how welfare is lost as the zonal market clearing problem gets too restrictive. On the other hand, other parts of the same feasible region can be too loose, which can entail the need for redispatch. The cost-efficiency of this redispatch process is eventually called into question, again causing welfare losses. Even though various researchers rightly acknowledge the relevance of redispatch (e.g. [Matthes et al., 2019; Schönheit et al., 2020]), the interplay of FBMC-style constraints and redispatch has so far not been investigated.<sup>2</sup>

This article is structured as follows: Section 2 provides a summary of the theoretical background. It explains the equations describing the physical constraints of the power system and the load flow constraints considered under FBMC compared to a nodal market design. Subsequently, Section 3 presents the framework for a stylized analysis conducted in Section 4 which illustrates the implications of the essential elements of the FBMC methodology, and Section 5 provides a numerical example which includes a quantification of welfare. Thereafter, Section 6 draws the relevant conclusions.

## 2. European FBMC vs nodal market design

From an economic point of view, the maximization of social welfare is generally seen as the key objective when designing electricity markets. In the absence of price elasticity of demand, maximizing welfare corresponds to an optimization problem that minimizes operational system costs under several constraints.<sup>3</sup>

This statement equally holds for nodal and zonal market designs. However, in terms of formulating the constraints of power flows through the electricity grid (i.e., load flow constraints (LFCs)), both market designs differ substantially. The conceptual differences are explained subsequently. We start with the nodal market because it yields welfare-optimal market outcomes.<sup>4,5</sup>

<sup>2</sup> One exception in this regard is constituted by [Voswinkel et al., 2019], a work which has partly been built on the findings of this paper.

<sup>3</sup> Note that we make the assumption of inelastic demand throughout this paper. Therefore, we do not define the utility of demand. Furthermore, we always use the term “social welfare” under this assumption.

<sup>4</sup> Note that the nodal model as discussed here also includes “some simplifications or put differently abstracts from” real-world phenomena. These include notably the non-linear AC power flow equations which are replaced by the approximation through PTDFs. Also N-1 security constraints are disregarded as well as possibilities of grid topology changes that may exist in real-world networks. Yet all these elements may be integrated in nodal network models (and at least partly also in zonal models). But their inclusion does not fundamentally alter the subsequent analyses, therefore they are omitted here for more clarity. We will further comment on the effect of the N-1 criterion in section 6.

<sup>5</sup> A wide variety of terminology is used in literature and reports from various institutions that describe FBMC. Some terms are used interchangeably, while not necessarily referring to the same parameters. It is important to be aware of these differences. For an introduction to the most-used terms, the reader is referred to [Van den Bergh et al., 2016].

2.1. Representation of physical behavior of line loads and restrictions – The nodal market design

The nodal electricity market clearing problem (EMCP) is given in Eqs. (1)–(5). Therein, Eq. (1) represents the objective function, and  $g_i$  is the aggregate generation at each grid node  $i$ .  $c_i$  are the corresponding marginal costs at node  $i$ . We assume the marginal costs of each generator to be constant. In terms of aggregate nodal generation  $g_i$  (i.e., several generators), the marginal costs may thus be described by a step function  $c_i(g_i)$ . The symbol  $I$  represents the set of all nodes of the system, while  $\Delta t$  denotes the time step. Eq. (2) represents the LFCs. Here,  $A_{f,i}$  is the power transfer distribution factor (PTDF) for the loading of line  $f$  resulting from an exchange from node  $i$  to an (arbitrary) reference node.<sup>6</sup>  $C_f$  is the line capacity.  $q_i$  is the net export at node  $i$ , which is simply the balance of generation  $g_i$  and demand  $d_i$  (Eq. (3)). The solution to the optimization problem remains unchanged if non-binding lines are removed from the set of considered lines  $F_x$ . The resulting set of relevant lines  $F_x$  includes all lines whose capacity restriction becomes binding at least in one situation. Eq. (4) ensures that generation and demand of the overall system are in balance, Eq. (5) expresses the capacity constraints of the generators.

$$\min_{g_i} \sum_{i \in I} \int_0^{g_i} c_i(g_i) dg \Delta t \quad (1)$$

$$s.t. \quad -C_f \leq \sum_{i \in I} A_{f,i} q_i \leq C_f \quad \forall f \in F_x \quad (2)$$

$$q_i = g_i - d_i \quad \forall i \in I \quad (3)$$

$$\sum_{i \in I} q_i = 0 \quad (4)$$

$$0 \leq g_i \leq g_i^{\max} \quad \forall i \in I \quad (5)$$

Eqs. (1)–(5) constitute a nodal EMCP. Moreover, as the LFCs of this nodal EMCP (Eq. (2)) consider the actual line loading behavior quite precisely, they can be regarded as physical grid constraints. These nodal LFCs always need to be fulfilled – no matter if the market design is nodal or zonal.

2.2. Zonal pricing using FBMC

For understanding FBMC, it is important to be aware of the sequential character of FBMC. Fig. 1 illustrates the main stages of the FBMC process. Two days before delivery (D-2), the capacity allocation takes place, i.e., the TSOs determine the parameters which define how much cross-zonal trade is allowable. These grid-based input parameters are used in the 2nd stage (D-1), when the day-ahead market is cleared. This clearing aims at the welfare-optimal use of available exchange capacities.

At D-1, the EMCP as shown in Eqs. (6)–(10) is solved. In contrast to section 2.1, we now assume that the system is composed of a set of price zones  $Z$ . Each zone  $z$  contains a set of nodes  $I_z$ . This optimization problem is quite similar to the nodal EMCP; i.e., the objective function,

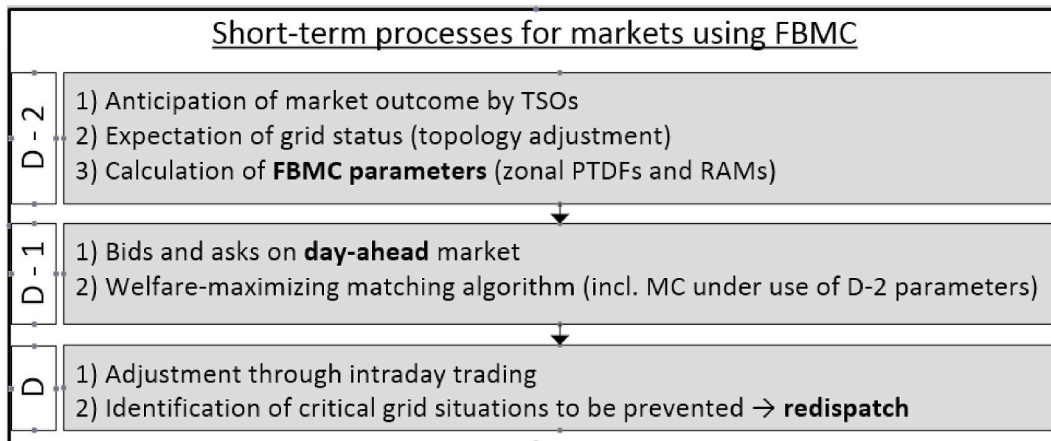


Fig. 1. Illustration of real-world processes and the corresponding modeling.

$$\min_{g_i} \sum_{i \in I} \int_0^{g_i} c_i(g_i) dg \Delta t \quad (6)$$

$$s.t. \quad R_f^{nsfd} \leq \sum_{z \in Z} \bar{A}_{f,z} \bar{q}_z \leq R_f^{sfd} \quad \forall f \in F_{cb} \quad (7)$$

$$\bar{q}_z = \sum_{i \in I_z} g_i - \sum_{i \in I_z} d_i \quad \forall z \in Z \quad (8)$$

$$\sum_{z \in Z} \bar{q}_z = 0 \quad (9)$$

$$0 \leq g_i \leq g_i^{\max} \quad \forall i \in I \quad (10)$$

<sup>6</sup> PTDFs express the line loading sensitivity in terms of net exports. We limit the illustration to the DC lossless load flow approximation (cf. [Zimmermann et al., 2011]).

system balance equation and capacity constraints of the generators remain unchanged. The main difference is that only the net exports at the level of price zones,  $\bar{q}_z$ , are taken into account (Eq. (8)) and, thus, only these are constrained (Eq. (7)), entailing three conceptual changes. First, the sensitivity of loading line  $f$  resulting from an exchange from zone  $z$  (instead of node  $i$  in the nodal design) to a reference node must be used. Accordingly, the PTDFs are used in their zonal form, denoted by  $\bar{A}_{f,z}$ . The second conceptual change is the use of remaining available margins (RAMs)  $R_f^{nsfd/sfd}$  as limit values in Eq. (7). The third difference is that constraints are only considered for a subset of lines  $F_{cb} \subseteq F$ .

The calculation of  $\bar{A}_{f,z}$  and  $R_f^{nsfd/sfd}$  as well as the choice of  $F_{cb}$  are discussed in the subsequent sections.

### 2.2.1. The zonal PTDF $\bar{A}_{f,z}$

For translating nodal to zonal PTDFs, certain approximations must be made. Key elements for calculating  $\bar{A}_{f,z}$  are the generation shift keys (GSKs)  $\lambda_{z,i}^{inc.(p)}$ .

$$\bar{A}_{f,z} = \sum_{i \in I_z} \lambda_{z,i}^{inc.(p)} A_{f,i} \quad \text{with} \quad \sum_{i \in I_z} \lambda_{z,i}^{inc.(p)} = 1 \quad (11)$$

Mathematically, the GSKs serve as weights when computing the zonal PTDF as a weighted average of the nodal PTDFs of the nodes included in the respective zone. By regarding Eqs. (2), (7) and (11), the role of GSKs becomes apparent: GSKs are used to distribute a change in net exports of a zone, denoted by  $\Delta \bar{q}_z$ , to nodes within that zone, i.e., to allocate changes in net exports to these nodes ( $\Delta \bar{q}_z \xrightarrow{GSK} \Delta q_i$ ). From Eq. (11), it is not straightforward why the allocation by means of GSKs refers to changes in zonal net exports (i.e.,  $\Delta \bar{q}_z$  to  $\Delta q_i$ ) instead of absolute net exports (i.e.,  $\bar{q}_z$  to  $q_i$ ). We come back to this point in the next paragraph.

### 2.2.2. The remaining available margin $R_f^{nsfd/sfd}$

The remaining available margins (RAMs) consist of four elements: the line capacity  $C_f$ , the expected line loading offset  $\Delta L_f^{(e)}$ , the flow reliability margin (FRM)  $M_f$  and the final adjustment value (FAV)  $V_f$ .<sup>7</sup> As power flows on transmission lines can have two directions, one direction has to be accounted positively. Thus, we distinguish between standard flow direction (SFD), which is defined to be positive, and non-standard flow direction (NSFD) being negative.<sup>8</sup>

$$R_f^{sfd} = C_f - \Delta L_f^{(e)} - M_f - V_f \quad (12)$$

$$R_f^{nsfd} = -C_f - \Delta L_f^{(e)} + M_f + V_f \quad (13)$$

The expected line loading offset  $\Delta L_f^{(e)}$  takes into account the difference of the expected line loadings in a nodal power flow model and in a zonal power flow model. The term ‘‘expected’’ refers to the nature of these line loadings. As opposed to considering actual power flows, the expected line loading offset is a term that is determined at the D-2 stage and, therefore, goes along with anticipated states of the power system at this point. More specifically, on the one hand,  $\Delta L_f^{(e)}$  considers the power flows that can be expected to result from the base case net exports  $q_i^{(e)}$  (i.e., expected power flows subject to an expected market clearing). Such a base case represents a best estimate of the power system for the day of delivery (D). We superscribe values that are dependent on this

base case expectation with  $(e)$ . If any of the expected  $q_i^{(e)}$ 's is non-zero, the expected line loading of at least one line is unequal to 0. The expected line loadings reduce the free line capacity. They are given by  $\sum_{i \in I} A_{f,i} q_i^{(e)}$ . On the other hand, the expected line loading offset  $\Delta L_f^{(e)}$  takes into account the expected power flows that would result from a zonal power flow approximation – thus again being subject to an expectation of the market clearing. The reason for that is straightforward: Using a base case also implies that changes in line loading result from deviations of zonal net exports from the base case (i.e., from  $\Delta \bar{q}_z = \bar{q}_z - \bar{q}_z^{(e)}$ ). However, Eq. (7) only contains  $\bar{q}_z$  in its inner term, since the expected part ( $\sum_{z \in Z} \bar{A}_{f,z} \bar{q}_z^{(e)}$ ) is shifted to the left and right side of Eq. (7). From the EMCP perspective, this part is constant (since it is predetermined) and, therefore, is contained in the RAMs. Thus,  $\Delta L_f^{(e)}$  is calculated as follows.

$$\begin{aligned} \Delta L_f^{(e)} &= \sum_{i \in I} A_{f,i} q_i^{(e)} - \sum_{z \in Z} \bar{A}_{f,z} \bar{q}_z^{(e)} \\ &= \sum_{z \in Z} \sum_{i \in I_z} A_{f,i} \left( q_i^{(e)} - \lambda_{z,i}^{inc.(p)} \bar{q}_z^{(e)} \right) \end{aligned} \quad (14)$$

The purpose of the base case can be explained best when observing its effect on the FBMC domain. Therefore, we wait with its explanation until section 4.2. However, its use is the reason for the incremental character of GSKs, i.e., why GSKs map incremental changes ( $\Delta \bar{q}_z = \bar{q}_z - \bar{q}_z^{(e)} \xrightarrow{GSK} \Delta q_i = q_i - \bar{q}_i^{(e)}$ ). This issue becomes clear when inserting Eq. (12) together with Eq. (14) and Eq. (11) into the LFC in SFD in Eq. (7). After slight rearrangements, this then reads:

$$\begin{aligned} &\sum_{z \in Z} \sum_{i \in I_z} A_{f,i} \lambda_{z,i}^{inc.(p)} \left( \bar{q}_z - \bar{q}_z^{(e)} \right) \\ &\leq C_f - \sum_{i \in I} A_{f,i} q_i^{(e)} - M_f - V_f \end{aligned} \quad (15)$$

In almost all of the cases, this incremental characteristic makes it reasonable to limit  $\lambda_{z,i}^{inc.(p)}$  to positive values; that is it would be strange to expect generators at a node to decrease their generation while the overall generation in that zone increases.<sup>9,10</sup> Notably, the resulting range from 0 to 1 for all GSKs is also respected by procedures in public GSK guidelines (cf. section 2.2.5).

### 2.2.3. FRMs and FAVs

The third term for calculating the RAM is the FRM. For now, it is sufficient to note that FRMs exist, i.e., some sort of margin that can only make zonal LFCs more restrictive ( $M_f \geq 0$ ). Its motivation and a numerical example are provided in section 4.5. The FAVs are partly different. They can be positive, accounting for the additional risk of overload, or negative, accounting for complex remedial actions (cf. [Amprion et al., 2014]). Positive FAVs act identically to FRMs. Negative FAVs are very specific to the set of available control elements of the grid. FAVs are not included in the aforementioned ‘‘non-resolvable complexities’’ of FBMC (cf. [Entso-E, 2018]) and, therefore, not in the focus of this paper. However, we briefly comment on this aspect in section 4.4.

### 2.2.4. Considered lines

As stated in sec. 2.2, in FBMC, constraints are only applied for a subset of transmission lines  $F_{cb} \subseteq F$ . The subset  $F_{cb}$  contains all inter-zonal

<sup>7</sup> Note that we neglect reference flows that may be considered to account for commercial transactions outside of the day-ahead market (e.g., long-term nominations from the forward markets, cf. [Van den Bergh et al., 2016]). This simplification does not change the general conclusions of this paper. As a matter of fact, also the magnitude of long-term nomination has significantly reduced in practice over the last years.

<sup>8</sup> Note that this is simply a matter of convention but must be consistent.

<sup>9</sup> Note that there are exceptional cases in which negative GSKs may be reasonable. For instance, these cases can be a result of anticipation of negative redispach of a certain power plant/at a certain node.

<sup>10</sup> In terms of the demand, the reason for limiting  $\lambda_{z,i}^{inc.(p)}$  at 0 and 1 is the high spatial correlation of main drivers of electric demand (cf. [Xie and Hong 2016; Ziel and Liu 2016]).

lines and some intra-zonal lines. TSOs have determined a threshold for considering intra-zonal lines: If the maximum zone-to-zone PTDF<sup>11</sup> of a line is higher than 0.05, the line is considered to be significant (cf. [Amprion et al., 2014]).

### 2.2.5. TSO procedures for D-2 calculations

All of the aforementioned FBMC elements, namely GSKs  $\lambda_{z,i}^{(p)}$ , base case and resulting  $\Delta L_f^{(e)}$ , FRMs, FAVs and the set  $F_{cb}$  of considered lines, must be determined at the D-2 stage, or earlier. TSOs have published several procedures and guidelines in this regard. In terms of GSKs, [Entso-E, 2016] proposes relatively unsophisticated calculation methods.<sup>12</sup> For instance, GSKs can be calculated being proportional to the base case generation, proportional to remaining available capacities or depending upon a merit order list. In practice, other calculation methods are used. Most frequently, GSK values reciprocal to the number of nodes in a zone or proportional to installed capacities are encountered in practice (cf. [Dierstein 2017]).<sup>13</sup> We consider all of these procedures to be rule-based rather than representing an expectation. Therefore, we superscribe the GSK parameters – as used in FBMC – with  $(p)$  for “pre-determined” instead of  $(e)$  for “expected”.

The determination of the base case is described in [Amprion et al., 2014] and [Elia, 2015]. In short, participating TSOs elaborate 2-day-ahead congestion forecasts. These represent best estimates of the state of the power system at day D. Several of the input parameters are taken from an agreed reference day (e.g., net exchange programs, generation of units) and are adjusted according to, amongst others, load, renewables and outage forecasts.

## 3. Considered case

For showing the effects of all FBMC elements, we consider the stylized 4-node examples shown in Fig. 3. The physical system in both figures is identical (cf. line properties in Table 1 and resulting PTDFs in Table 2). The only difference is the market design. In Fig. 2, it is a nodal pricing design, i.e., each node constitutes a separate price zone. In Fig. 3, nodes 2 and 3 are assigned to one common zone BC. Here, zonal pricing using the FBMC approach is supposed (cf. Eqs. (6)–(14)).

For considering the welfare effects of zonal market clearing compared to nodal market clearing, we furthermore specify the load and generation characteristics given in Table 3. These values imply that the load centers are located at nodes 1 and 4. Relatively low-cost generation capacities are located at nodes 2 and 3 (zone BC). For the wind farm located at node 2, we distinguish between two cases: Case A representing times with sufficient wind to generate 300 MW of electricity; case B assuming no wind (section 5). The second low-cost generation alternative, a coal-fired power plant, is placed at node 3. There are also

**Table 1**  
Line properties for the chosen example.

line $f$ :	$\alpha$	$\beta$	$\gamma$	$\delta$	$\epsilon$
line capacity $C_f$ [MW]:	75	75	130	50	130
line resistance $[\Omega]$ :	50	50	50	50	50

<sup>11</sup> A zone-to-zone PTDF is given by  $\bar{A}_{f,z} - \bar{A}_{f,z'}$  for two zones  $z$  and  $z'$ .

<sup>12</sup> Note that this statement solely refers to the mathematical formulation of GSKs. Of course, the topic as such is complex, especially because there is no clear consensus on which procedure works best in the sense of reducing redispatch and costs. In addition, certain GSK calculation methods may require the base case expectation, which again introduces complexity to the overall process.

<sup>13</sup> Note that statistical procedures were proposed recently (cf. [Schönheit and Sikora 2018]). However, they have yet to be validated and tested.

three gas-fired power plants located at nodes 1, 2 and 4. When using a capacity-weighted GSK approach,<sup>14</sup> the GSK at node 2 is 0.8.

## 4. Analyzing feasible regions and the impact of FBMC design elements

In order to analyze the impact of zonal market clearing and specific FBMC design elements, we first discuss some concepts and conventions helpful for the analysis. We then address the various design elements and their impacts on the feasible region (FRs) one by one - highlighting how differences with the nodal benchmark solution arise which potentially induce welfare losses. The welfare effects are then quantified for a specific set of load and generation characteristics in section 5.

### 4.1. Concepts and conventions for the analysis

For all explanations in the subsequent sections, we assume infinite power plant capacities (i.e., Eqs. (5) and (10) are non-binding). Our focus is on situations with limited exchange capacities (i.e., at least one binding LFC). In the subsequent analysis, we directly choose the point of welfare-optimal dispatch instead of deriving it from the cost minimization. This choice is appropriate as the differences between the zonal and nodal dispatch solely result from the distinct grid constraints of the corresponding EMCPs (cf. Eqs. (2) and (7)).<sup>15</sup> In this respect, the types of deviations of the zonal constraints from their nodal counterparts are described in full. The FRs are subsequently shown in the  $q_1$ - $q_4$  plane. With the zonal EMCP containing three variables  $q_1$ ,  $q_4$  and  $\bar{q}_{BC}$ , out of which only two are independent due to Eq. (9), the zonal FR is fully defined in the  $q_1$ - $q_4$  plane.<sup>16</sup> The nodal EMCP contains three free export variables. Therefore, only subspaces of the nodal FR can be depicted unequivocally in any 2D illustration. Before explaining the way of defining these subspaces, we introduce the following definitions:

- $\lambda_{z,i}^{inc.(p)}$ : The incremental and predetermined GSK as used in FBMC (cf. section 2.2.1 and 2.2.2).
- $r_{z,i}^{abs.(e)}$ : The expected net export ratio (NER), i.e., the ratio of nodal to zonal net exports. The term “expected” indicates that the NER is (implicitly) given by the base case expectation. Thus,  $r_{z,i}^{abs.(e)}$  is equal to  $\frac{q_i^{(e)}}{\bar{q}_z^{(e)}}$ .
- $r_{z,i}^{abs.(r)}$ : The realized NER. The term “realized” points to an ex-post perspective. Knowing the result of an EMCP allows calculation of the realized NER. It can be constructed from any feasible solution of the nodal EMCP with  $\bar{q}_z \neq 0$ .
- $\lambda_{z,i}^{inc.(r)}$ : The incremental realized GSK. Again, we use an ex-post perspective. In contrast to  $r_{z,i}^{abs.(r)}$ ,  $\lambda_{z,i}^{inc.(r)}$  is now calculated using the deviations of net exports from the base case expectation, i.e.,  $\lambda_{z,i}^{inc.(r)}$  being equal to  $= \frac{q_i^{(r)} - q_i^{(e)}}{\bar{q}_z^{(r)} - \bar{q}_z^{(e)}}$ .

<sup>14</sup> Only market-driven capacities are considered (i.e., no wind infeed is considered).

<sup>15</sup> This statement refers to the optimization problems as set up in Eqs. (1)–(5) and Eqs. (6)–(10). It should be noted that there are other ways of formulating zonal clearing problems. For instance, [Aravena Solis, 2019] formulate a zonal clearing problem under consideration of an exact projection of the grid. Such problems can – and in the case of [Aravena Solis, 2019] do – yield clearing results different to the nodally organized market for reasons different to grid constraints.

<sup>16</sup> Note that this aspect significantly distinguishes our illustrations from common TSO-style depiction (e.g., in [Plancke et al., 2016]), which depict subspaces of the zonal FR in terms of bilateral exchanges.

**Table 2**

PTDFs with reference node 3 (positive flow direction (SFD) going to the node with higher numeral,  $\bar{A}_{f,BC}$  for  $\lambda_{BC,2}^{inc,(p)} = 0.8$ ).

export at node	1	2	3	4	from zone	A	BC	D
$A_{\alpha,i}$ [-]	0.5	-0.125	0	0.125	$\bar{A}_{\alpha,z}$	0.5	-0.1	0.125
$A_{\beta,i}$ [-]	0.5	0.125	0	-0.125	$\bar{A}_{\beta,z}$	0.5	0.1	-0.125
$A_{\gamma,i}$ [-]	0.5	0.625	0	0.375	$\bar{A}_{\gamma,z}$	0.5	0.5	0.375
$A_{\delta,i}$ [-]	0	0.25	0	-0.25	$\bar{A}_{\delta,z}$	0	0.2	-0.25
$A_{\epsilon,i}$ [-]	-0.5	-0.375	0	-0.625	$\bar{A}_{\epsilon,z}$	-0.5	-0.3	-0.625

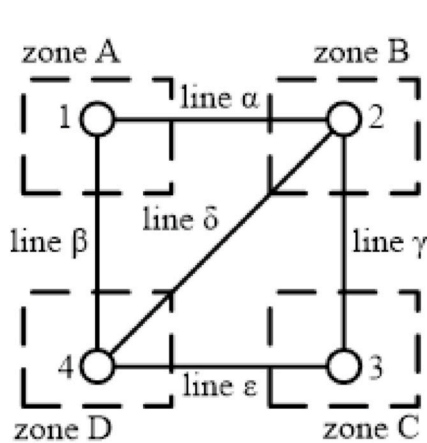


Fig. 2. Stylized example under a nodal pricing regime.

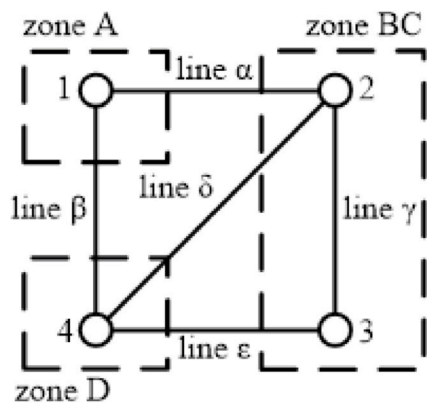


Fig. 3. Stylized example under a zonal pricing regime.

**Table 3**

The situation of the power system.

node $i$	demand $d_i$	installed technology	available generation capacity $g_i^{max}$	variable costs $c_i$
1	150 MW	gas-fired power plant	150 MW	70/MWh
2	0 MW	gas-fired power plant	1200 MW	50/MWh
		wind farm	case A: 300 MW case B: 0 MW	0/MWh
3	0 MW	coal-fired power plant	300 MW	40/MWh
4	150 MW	gas-fired power plant	150 MW	70/MWh

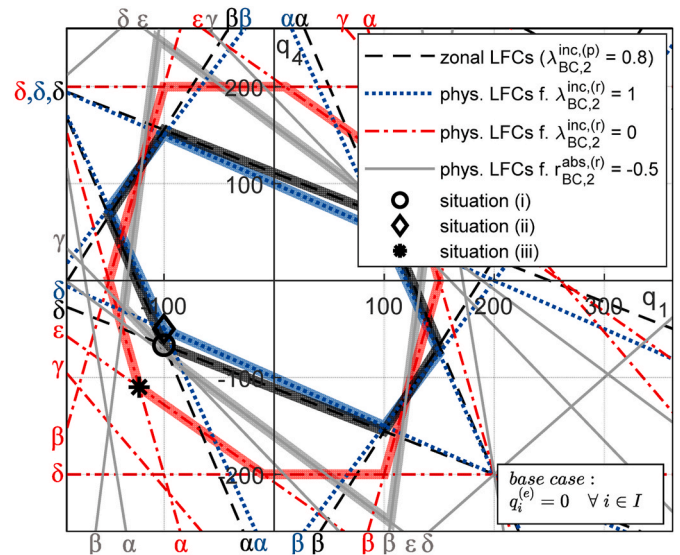


Fig. 4. LFCs of the zonal and nodal EMCP for the 4-node example under a zero base case (for the nodal EMCP, three realizations are shown).

As explained,  $\lambda_{z,i}^{inc,(p)}$  typically ranges from 0 to 1. For all our examples, we arbitrarily choose  $\lambda_{BC,2}^{inc,(p)} = 0.8$ .<sup>17</sup> In turn, NERs and  $\lambda_{BC,2}^{inc,(r)}$  may also take values greater than 1 or less than 0, which is further described in section 4.2. Notably, the last three parameters ( $r_{z,i}^{abs,(e)}$ ,  $r_{z,i}^{abs,(r)}$  and  $\lambda_{z,i}^{inc,(r)}$ ) are no parameters used in FBMC procedures. Both realized values,  $\lambda_{BC,2}^{inc,(r)}$  and  $r_{BC,2}^{abs,(r)}$ , are introduced in this paper for defining subspaces of the nodal FR. We have chosen to use these elements because of their mathematical similarity to  $\lambda_{BC,2}^{inc,(p)}$ . However, it is important to note that the GSK  $\lambda_{BC,2}^{inc,(p)}$  is the only parameter used in FBMC. In particular, neither  $\lambda_{BC,2}^{inc,(r)}$  nor  $r_{BC,2}^{abs,(r)}$  are defined ex ante and do not impose any restriction to the nodal FR. That is, the actual nodal FR is composed of a multitude of subspaces like those being illustrated subsequently. Furthermore,  $\lambda_{BC,2}^{inc,(r)}$  is computed with reference to a base case. However, the base case concept does not exist in nodal designs, as solving the nodal EMCP is done in one single step. Thus,  $\lambda_{BC,2}^{inc,(r)}$  and  $r_{BC,2}^{abs,(e/r)}$  are concepts exclusively used for visualization, which ought not be confused with reduced flexibility of the nodal EMCP. Along the same lines,  $r_{z,i}^{abs,(e)}$  is a metric to describe the base case. It could equally be determined for real-world base cases, but TSOs typically do not use this metric.

<sup>17</sup> This corresponds to the capacity-weighted GSK approach given the thermal capacities outlined in Table 3.

#### 4.2. Use and effect of GSKs

In order to analyze the influence of GSKs, we start by considering the base case  $(e)_0$  being defined as  $q_i^{(e)} = 0 \forall i \in I$ .<sup>18</sup> Fig. 4 describes the constraints imposed in the energy market clearing problems for the example described in section 3. As discussed in the previous section, the illustration is done in a  $q_4 - q_1$  plane. The black dashed lines in Fig. 4 represent the load flow constraints (LFCs) of the zonal EMCP with the assumed GSK  $\lambda_{BC,2}^{inc.(p)} = 0.8$ . The parts of the LFCs which define the zonal FR are highlighted in bold and black. To illustrate the possible outcomes of a nodal EMCP, we consider two possible realizations of  $\lambda_{BC,2}^{inc.(r)}$ : 0 (red and dash-dotted) and 1 (blue and dotted). That is, ex post, the optimal (marginal) share of generation in node 2 differs from the ex-ante assumed GSK of 0.8. The corresponding subspaces of the nodal FR are highlighted in bold using the same color scheme as for the corresponding LFCs.

In Fig. 4, we also point to the specific exchange situations (i) to (iii), which we discuss subsequently. Assume that the solution of the zonal EMCP corresponds to situation (i). In a nodal EMCP, the welfare-optimal solution may be different. Such a solution can be described by  $q_1, q_4, (e)_0$  and  $\lambda_{BC,2}^{inc.(r)}$ . Then, any deviation of  $\lambda_{BC,2}^{inc.(r)}$  from  $\lambda_{BC,2}^{inc.(p)}$  changes the optimal feasible exchange. Subsequently, we discuss the expected solution, the two further possible GSK realizations and the consequences of their divergence:

**Zonal solution with  $\lambda_{BC,2}^{inc.(p)} = 0.8$ :** The solution of the zonal EMCP is given at  $\bar{q}_{BC} = 166.7$  MW, which corresponds to  $q_1 = -100$  MW and  $q_4 = -66.7$  MW (situation (i) in Fig. 4). At this point, lines  $\alpha$  and  $\delta$  are expected to be entirely loaded (and therefore of most interest in terms of market clearing results). If  $\lambda_{BC,2}^{inc.(r)}$  is identical to the expectation (0.8), then situation (i) also represents the nodal solution in our stylized example. Thus, the zonal solution would be welfare-optimal, and redispatch is not required on the day of delivery.

**$\lambda_{BC,2}^{inc.(r)} = 1$ , i.e., all net exports of zone BC stem from node 2:**  $q_2$  has a stronger impact on both most relevant line loadings (of lines  $\alpha$  and  $\delta$ ) than  $q_3$ . Therefore, the zonal solution ( $\bar{q}_{BC} = 166.7$  MW) breaches either one or both of these technical constraints ( $\alpha$  and/or  $\delta$ ). Hence, the solution of the zonal EMCP would make redispatch necessary. Assume that the optimal solution under adequate consideration of technical constraints would then be the one given at situation (ii), i.e.,  $q_1 = -100$  MW,  $q_4 = -50$  MW and, thus,  $\bar{q}_{BC} = 150$  MW. Taking the zonal solution as a starting point (as it is the outcome of the D-1 stage under FBMC, cf. item a)), the optimal solution (ii) could only be achieved by negative redispatch at node 2 and positive redispatch at node 4. Alternatively, technical feasibility could be established by intra-zonal redispatch at nodes 2 and 3. However, this alternative redispatch will not yield a welfare-optimal result. Thus, resulting welfare depends on the way redispatch is performed. Section 5 provides various options for performing redispatch and explains why inefficiencies are most likely – even when given a simple 4-node example.

**$\lambda_{BC,2}^{inc.(r)} = 0$ , i.e., all net exports of zone BC stem from node 3:** As  $q_3$  has a weaker impact on both most relevant line loadings than  $q_2$ ; higher net exports from zone BC would be permissible. The set of relevant lines even changes (from  $\alpha$  and  $\delta$  in situation (i) to  $\alpha$  and  $\varepsilon$  in situation (iii)). Again, the solution of the zonal EMCP (situation (i)) is suboptimal – in

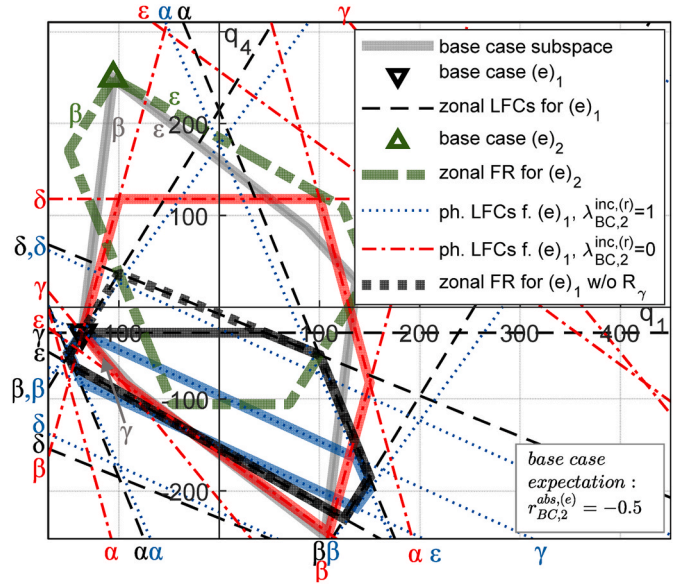


Fig. 5. LFCs of the zonal and nodal EMCP for the 4-node example under a non-zero base case (for the nodal EMCP, two realizations are shown for base case  $(e)_1$ ; for base case  $(e)_2$ , LFCs are not shown for lucidity).

this case, because some available line capacities remain unused.

For different market situations, the direction of exchanges and, correspondingly, the point of highest welfare may be different. However, in the case of constrained exchange capacities, the effects of GSK inaccuracies will be throughout similar to the ones described above. For quantification of welfare losses, the reader is referred to section 5.

In Fig. 4, we also show physical LFCs for  $r_{BC,2}^{abs.(r)} = -0.5$  (grey solid lines). A negative NER can occur, for instance, when some nodes in a zone are net exporters (e.g., surplus of low-cost generation capacities) while other nodes in the same zone are net importers (e.g., no generation capacities). If the zonal net export is positive, this results in a negative NER for the importing node. Implicitly, part of the generation at the exporting nodes is balanced with the demand at the importing nodes, which is equivalent to (implicit) intra-zonal trade. In the regarded case, most of the electricity traded between node 3 and 2 is transmitted through the intra-zonal line  $\gamma$ , thereby reducing its free capacity for cross-zonal trade.<sup>20</sup> A smaller part takes indirect routes through the grid.

Even if all zonal net exports are 0, lines may be loaded if there are exchanges between nodes within one zone. As indicated by the PTDF matrix, there will then also be flows through other parts of the grid – these are the so-called loop flows [Elia, 2017]. The inner term of Eq. (7) does not take into account intra-zonal trade. Yet, their impact on the line loadings is contained in the term  $\Delta L_f^{(e)}$ . Describing the impact of intra-zonal trade on line loadings is hence one major purpose of the base case, which is elaborated on subsequently.

#### 4.3. Use and effect of the base case

Following the previous considerations, we now relax the initial assumption of all  $q_i^{(e)}$  being equal to 0. As explained above, the base case is suited for taking into account anticipated (intra-)zonal trade. We arbitrarily choose situations with intra-zonal trade as possible base cases. We know from section 4.2 that  $r_{BC,2}^{abs.(e)} = -0.5$  describes such

<sup>18</sup> This is an assumption that abstracts from the real world. In actual practice, this would mean that TSOs expected the market result to be balanced at each grid node. As there are always differences in marginal costs within a system and as supply capacities at certain nodes are typically not sufficient to meet the nodal demand, this expectation would lack justification. However, we make this assumption in order to decompose the effect of the different FBMC elements.

<sup>19</sup> Note that  $r_{BC,2}^{abs.(r)}$  is equal to  $\lambda_{BC,2}^{inc.(r)}$  when using the base case  $(e)_0$ .

<sup>20</sup> More specifically, PTDFs in Table 2 show that transmission through line  $\gamma$  corresponds to 62.5% of traded volumes between nodes 3 and 2. Thus, the LFCs of line  $\gamma$  can become relevant (i.e., possibly binding) for situations with  $r_{BC,2}^{abs.(r)} = -0.5$ , as can be seen in Fig. 4.

situations. Thus, we choose two situations that lay within the subspace of the nodal FR for this NER. This base case subspace is highlighted in grey in Fig. 5 for reference.

The chosen base cases are denoted by  $(e)_1$  and  $(e)_2$  (indicated by the two triangles).<sup>21, 22</sup> These base cases, together with the predetermined GSK  $\lambda_{BC,2}^{inc.(p)}$  entirely define the zonal FRs. These zonal FRs are marked by the solid black  $((e)_1)$  and dashed green  $((e)_2)$  enframed areas. They can be understood as planar cuts through the nodal FR (feasibility polyhedron). The tilt of these planar cuts is defined by  $\lambda_{BC,2}^{inc.(p)}$ . The offset from the origin is given by  $(e)_1$  and  $(e)_2$ , respectively. Thus, the base case, by design, constitutes one situation in the nodal and in the zonal FR. In our examples, the base cases are located at the corners of the nodal FR defined by the LFCs of line pairs  $\beta/\gamma$  and  $\beta/\epsilon$ . The corresponding LFCs are also binding in the zonal EMCP if and only if the market outcome is identical to the base case situation. Thus, if the base case represents (or, at least, is close to) the welfare-optimal dispatch situation, this welfare-optimal situation (or situations close to the welfare optimum) is part of the zonal FR.

By comparison of the zonal FRs of  $(e)_1$  and  $(e)_2$ , it becomes apparent that the zonal FRs depend on the base case in terms of relevant LFCs, size of FRs and differences of feasible sets. It is evident that the accuracy of the base case expectation is a prerequisite for good FBMC results.

Fig. 5 also shows the LFCs for  $(e)_1$  when realized GSKs differ from  $\lambda_{BC,2}^{inc.(p)}$  (using the same color scheme as in Fig. 4). As in section 4.2, the subspaces of the nodal FR are quite different. In particular, the subspace for  $\lambda_{BC,2}^{inc.(r)} = 0$  is much wider than the zonal FR, which illustrates the increased flexibility available to the nodal EMCP due to more degrees of freedom.

As before, the zonal EMCP may hence either lead to welfare losses compared to the nodal case or require redispatch.

#### 4.4. Considering intra-zonal lines

In base case  $(e)_1$  in section 4.3, one of the LFCs of the intra-zonal line  $\gamma$  is binding (cf. Fig. 5). From section 4.3, we know that this LFC is also relevant for the definition of the zonal FR. If  $\lambda_{BC,2}^{inc.(r)}$  is equal to  $\lambda_{BC,2}^{inc.(p)}$ , any dispatch situation with  $q_4 > -27.85$  MW will lead to overloads of line  $\gamma$ . If the LFC of line  $\gamma$  is not considered, the zonal FR allows  $q_4$  to exceed this limit. This is illustrated by the alternative zonal FR, enframed by bold and black dotted lines. Thus, considering LFCs of internal lines can help to avoid overload situations. Nevertheless, the recourse of the zonal EMCP to prevent such overloads is limited, since only zonal net exports can be optimized, although the more effective congestion management may be the optimization of intra-zonal trade. We subsequently use our example to illustrate this.

Consider the possible trades of 100 MWh from (a) node 4 to zone BC, (b) node 1 to zone BC and (c) node 3 to node 2. With the FBMC power flow approximation, i.e.,  $\lambda_{BC,2}^{inc.(p)}$ , trades (a) and (b) result in a change of transmitted electricity through line  $\gamma$  of  $-12.5$  MWh and  $0$  MWh, respectively (cf.  $A_{\gamma,1/4} - \bar{A}_{\gamma,BC}$ ). By contrast, the intra-zonal trade (c) changes transmission through line  $\gamma$  by  $62.5$  MWh ( $A_{\gamma,3} - A_{\gamma,2}$ ). Even though intra-zonal adjustments are the most effective way of managing congestion on line  $\gamma$ , the zonal EMCP can only optimize zonal net exports (i.e. only being able to steer trades (a) and (b) instead of trade (c)).

Analogously, the high  $A_{\gamma,2}$  entails that the LFC for line  $\gamma$  is extremely sensitive to the intra-zonal trade expected in the base case. The above

<sup>21</sup> Note that the base cases  $(e)_1$  and  $(e)_2$  do not correspond to the values in Table 3. Having such base case expectations would imply much different expectations in terms of demand and variable costs. As we use these base cases for methodological scrutiny only, we do not specify the corresponding nodal demand nor the variable costs further.

<sup>22</sup> Quantitative descriptions of the base cases are presented in appendix A.

example shows that 1 MWh of additionally expected trade from node 3 to 2 limits the exports from node 4 by additional 5 MWh. Hence, a tight upper bound of the net exports at node 4 is implemented in the zonal EMCP.

The previous statement notably holds for the effect of forecast deviations on intra-zonal trades in the base case. However, it likewise constitutes a dilemma for any base case expectation with binding or even overloaded intra-zonal lines. If the true expectation of intra-zonal trades is high, the base case yields either a highly constrained or empty zonal FR. This situation would either imply welfare decreases or make day-ahead clearing infeasible. If the base case is adjusted to contain less intra-zonal trade, the zonal FR is less restrictive, but the zonal market clearing will result in higher intra-zonal trade (close to the true base case expectation). Thus, redispatch is the consequence. Such base case adjustments correspond to the implicit remedial actions mentioned in TSO documents [Elia, 2015]. However, these documents address the consideration of implicit remedial actions quite vaguely and merely state that these actions can be considered as FAV. The case described above gives a concrete example of the cause and effect of considering remedial actions in the base case.

Thus, two extreme positions regarding intra-zonal lines may be distinguished. Either they are disregarded in the zonal EMCP. Then, congestion management of these lines is not performed during the D-1 stage, which may require redispatch afterwards. Or intra-zonal lines are explicitly considered in FBMC, yet then they may strongly impede cross-zonal trade. In some cases, the impediments are so great that base case adjustments are necessary. These adjustments at the D-2 stage then materialize as redispatch on day D. Between these extreme positions, also intermediate solutions may be chosen, namely to include only some intra-zonal lines as constraints in the EMCP. Here, the example illustrates a prerequisite for meaningful inclusion of intra-zonal line constraints: that the corresponding power flows are sufficiently sensitive to variations in cross-zonal trade (cf. section 2.2.4 for the threshold established by TSOs).

#### 4.5. Use and effects of FRMs

In order to consider the uncertainties of the FBMC process, Entso-E procedures consider the incorporation of FRMs [Amprion et al., 2014], which have already been briefly introduced in section 2.2. By construction, an FRM causes a parallel shift of the zonal LFCs reducing the FR. For the sake of clarity, we now move back to our example in section 4.2 (base case  $(e)_0$ ). Furthermore, we suppose that redispatch is to be avoided altogether. Under this presumption, FRMs need to be chosen in a way that the zonal FR only contains technically feasible solutions. If we assume possible realizations  $\lambda_{BC,2}^{inc.(r)} \in [0, 1]$ , FRMs need to be chosen in a way that they shift the LFCs to the most critical realization. Fig. 6 illustrates the resulting FR of the zonal EMCP with FRMs (still assuming  $\lambda_{BC,2}^{(e)} = 0.8$ ). For brevity, we only contrast the zonal FR to the subspace of the nodal FR for  $\lambda_{BC,2}^{inc.(r)} = 0$  in Fig. 6. However, for the derivation of required FRMs, we have also taken into account  $\lambda_{BC,2}^{inc.(r)} = 1$ .

The red areas highlight solutions of the zonal EMCP which, without consideration of FRMs, would be technically infeasible at  $\lambda_{BC,2}^{inc.(r)} = 0$ . All blue areas depict the set of technically feasible solutions which, due to the zonal market design, are not part of the FR of the zonal EMCP. Thereof, the solutions indicated by dark blue areas (FR reduction 1) are excluded due to the distortion of the zonal FR compared to the nodal subspace. The solutions in the light blue areas are excluded due to the use of FRMs. FR reduction 2 is due to required contingency margins in case of  $\lambda_{BC,2}^{inc.(r)} = 0$ , FR reduction 3 is due to making provision for  $\lambda_{BC,2}^{inc.(r)} = 1$ . If the optimal solution of the nodal EMCP is located in any of the blue areas, this will cause a loss of welfare. More generally, even if the forecasts of the GSKs and of the market outcome were perfect, the

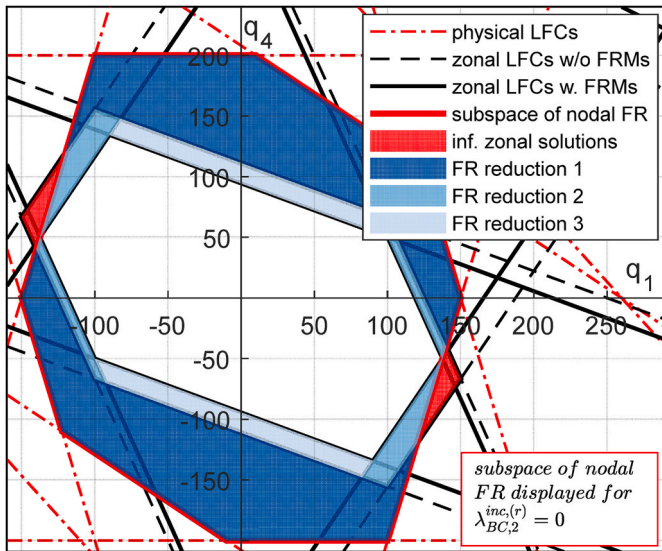


Fig. 6. LFCs of the zonal and nodal EMCP for the 4-node example under a zero base case (for the nodal EMCP, only one realizations,  $\lambda_{BC,2} = 0$ , is shown).

result of the zonal EMCP would still be suboptimal as long as the optimal solution contains a congested line being subject to an FRM. In practice, FRMs are yet not chosen as to avoid all possible redispatch measures. TSOs rather perform a statistical analysis [Amprion et al., 2014]. However, the reduction of the FR happens analogously.

5. Welfare implications

In section 4, we have focused on the general types of deviations of zonal grid constraints from their nodal counterparts and derived the resulting FRs from physical grid properties. However, we have not yet quantified the economic outcomes. The points of welfare-optimal dispatch have been chosen by assumption. In order to provide further insights in terms of welfare effects, we now refer to the additional assumptions from Table 3. As mentioned in section 3, these assumptions comprise two different cases differing in terms of the generation at node 2.

**Zonal clearing (case A):** During times of wind, a zero-cost generation source is available. The zonal EMCP makes use of the wind farm up to the point where the zonal LFCs become binding.

**Zonal clearing (case B):** Without wind being available, the electricity generation through the coal-fired power plant is cheapest. The zonal EMCP makes use of this power plant up to the point where the zonal LFCs become binding.

In both cases A and B, the zonal EMCP yields the same solution in terms of zonal net exports. The maximum net export of zone BC is 166.7 MW; net exports at node 1 and 4 are -100 MW and -66.7 MW, respectively. Recall that this situation has already been denoted by (i) in Fig. 4.

**Nodal clearing (cases A and B):** The solution of the nodal EMCP under case A is given by situation (ii) in Fig. 4. The solution of the nodal EMCP under case B is given by situation (iii) in Fig. 4.

For the zonal and nodal clearings under both cases, Table 4 shows the economic outcomes of the zonal and nodal EMCPs.

The interpretation of case B is the easiest. The zonal case B yields market outcomes with unnecessarily high market clearing costs. Compared to the nodal solution, the additional costs – or in other words: welfare losses – are 2,175 €, i.e., an increase of around 15.5%. Notably, redispatch will not cure this situation, as the zonal market outcome is technically feasible, and as redispatch is not used for ex-post optimization.

The interpretation of case A requires a more detailed analysis.

Table 4 Economic outcomes of the zonal and nodal EMCPs.

	situation (i)		situation (ii)	situation (iii)
	zonal case A	zonal case B	nodal case A	nodal case B
$g_1$	50 MW	50 MW	50 MW	47.5 MW
$g_2$ (wind)	166.7 MW	0 MW	150 MW	40 MW
$g_2$ (gas)	0 MW	0 MW	0 MW	0 MW
$g_3$	0 MW	166.7 MW	0 MW	212.5 MW
$g_{BC} (= q_{BC})$	166.7 MW	166.7 MW	150 MW	252.5 MW
$g_4$	83.3 MW	83.3 MW	100 MW	40 MW
market clearing costs	9,333 €	16,000 €	10,500 €	13,825 €

Table 5 Scheduled line loading of zonal case A and line capacities.

	$\alpha$	$\beta$	$\gamma$	$\delta$	$\epsilon$
scheduled	-79.2 MW	-20.8 MW	29.2 MW	58.3 MW	29.1 MW
$C_j$	75 MW	75 MW	130 MW	50 MW	130 MW

Indeed, market clearing costs of the zonal clearing are lowest. However, we know from section 4.2 that the scheduled generation would entail line overloads. The zonal case A corresponds to the scheduled line loadings shown in Table 5.

Line  $\alpha$  is scheduled to be overloaded by 4.2 MW, line  $\delta$  by 8.3 MW. Thus, redispatch needs to be carried out.

**Redispatch options:** How might redispatch measures look? The transmission system operators (TSOs) responsible for zone A and zone BC will want to cure the overload on line  $\alpha$ , the TSOs responsible for zone D and BC will want to cure the overload on line  $\delta$ . The first measure is best achieved by increasing generation at node 1 and decreasing it at node 2; the second measure would involve nodes 4 and 2. However, in some cases, the regulator may protect RES and therefore establish RES curtailment as last resort. In such a case, generation at node 2 may not be reduced. Another option may be to only perform intra-zonal redispatch (i.e., adjusting generation at nodes 2 and 3). Table 6 provides an overview of these redispatch options.

In the considered example, measure 3), which consists of redispatching at only node 2 and 4, is the preferred solution. On the one hand, this measure does not only cure overloads of line  $\delta$ , it also cures the overload of line  $\alpha$ . On the other hand, this measure coincidentally establishes the welfare-optimal solution (with market clearing costs and redispatch costs summing to the costs of the nodal clearing: 9,333 € + 1,167 € = 10,500 €). However, such coincidences cannot be expected. The combined execution of redispatch rather calls for safety margins in the process, as different redispatch measures can adversely affect each other. This possibility is highlighted by the sufficiency column in Table 6 indicating whether the stated measures do or do not establish an admissible grid state. This column shows that only 2 of the redispatch options are appropriate. The safety margins associated with these interdependencies are likely to entail further welfare losses. Another example of redispatch causing welfare losses is given by the intra-zonal option (option 7). Here, welfare losses of 166 € would be the result (166 € = 9,333 € (zonal dispatch) + 1,333 € (redispatch) - 10,500 € (nodal dispatch)).

Doubts about the cost-efficiency of redispatch already arise for a system consisting of 4 nodes. In a realistic setting with thousands of nodes, performing redispatch to attain this first-best solution seems far from possible.

**Zonal clearing under knowledge of GSKs:** Note that the intuition in this regard may be that once the “correct” GSKs are considered for the capacity allocation, the EMCP would not entail the necessity for

**Table 6**  
Redispatch measures and costs.

measure	$\Delta g_1$	$\Delta g_2$	$\Delta g_3$	$\Delta g_4$	redispatch costs	sufficiency
1) curing $\alpha$	6.7 MW	-6.7 MW	0 MW	0 MW	467 €	no
2) curing $\alpha$ /RES protection	11.1 MW	0 MW	0 MW	-11.1 MW	0 €	no
3) curing $\delta$	0 MW	-16.7 MW	0 MW	16.7 MW	1,167 €	yes
4) curing $\delta$ /RES protection	-33.3 MW	0 MW	0 MW	33.3 MW	0 €	no
5) 1 & 3 combined	6.7 MW	-23.3 MW	0 MW	16.7 MW	1,633 €	no
6) 2 & 4 combined	-22.2 MW	0 MW	0 MW	22.2 MW	0 €	no
7) intra-zonal	0 MW	-33.3 MW	33.3 MW	0 MW	1,333 €	yes

redispatch. We use the market clearing results for cases A and B to illustrate that this is very unlikely. Under case A,  $\lambda_{BC,2}^{inc.(r)}$  is 1; under case B,  $\lambda_{BC,2}^{inc.(r)}$  is 0.158. We now set  $\lambda_{BC,2}^{inc.(p)}$  to these values (i.e., TSOs anticipating the nodal market outcome with perfect foresight) and call the corresponding new cases A' and B'. The results of case A' exactly correspond to the results of the nodal clearing under the conditions of A. Thus, the aforementioned intuition is right in this case.

The results for case B' are shown in Table 7. They show that line  $\epsilon$  would be overloaded. But why is this so? The explanation can be given by considering the information that is available to the optimizer of the nodal and the zonal EMCP. In the nodal solution of case B, the optimizer takes due account of the option of increasing the generation at the second-most economic plant while avoiding the violation of the LFCs of line  $\epsilon$ . This is important, as shifting generation from node 3 to node 2 can relieve congestion on  $\epsilon$  (when operating close to the optimal dispatch state). Thus, the generation at node 2 is increased to the amount necessary to keep power flows precisely at the permissible level. Despite knowing the optimal share between generation at nodes 2 and 3 at the stage of the capacity allocation and considering this information for predetermining the GSK, the zonal EMCP cannot manage this trade-off. The reason is that the same zonal PTDF is implicitly assigned to nodes 2 and 3. Therefore, the optimizer in the zonal EMCP decides on the generation share at nodes 2 and 3 solely based on variable costs, thereby opting for all generation stemming from node 3 (i.e., from the node with the cheaper generation capacity). From this example, the general rule can be derived that, whenever a nodal optimizer would yield a solution where power plants within one zone would not be dispatched according to the order of their variable costs for reasons of staying within the permissible state of the power grid, the zonal EMCP will entail redispatch. This condition is not given in case A'. However, in this regard, Case A' is hypothetical. In a close-to-real-world example [Voswinkel et al., 2019], have shown that considering the GSKs as they would be realized under a nodal clearing – even under perfect foresight – practically does not avoid redispatch. In large-scale systems, a nodal clearing in the order of the variable costs of the power plants within each zone is simply very unlikely.

**6. Conclusion**

In this paper, we have derived a stylized model to compare FBMC-style zonal pricing to its nodal counterpart. We have used this model

**Table 7**  
Outcomes of case B': EMCP with  $\lambda_{BC,2}^{inc.(p)} = 0.158$ , remaining conditions as in case B.

node	1	2	3	4	market clearing costs
generation	47.5 MW	0 MW	252.5 MW	0 MW	13.425 €
line	$\alpha$	$\beta$	$\gamma$	$\delta$	$\epsilon$
scheduled line load	-70 MW	-32.5 MW	-107.5 MW	37.5 MW	145 MW

to analyze the causes and effects of all essential FBMC elements as applied in CWE – namely, the GSKs, the base case and intra-zonal load flow constraints. Throughout the paper, we have assessed the effects of all these elements in terms of welfare resulting from the market clearing as well as from potential redispatch measures. We have been able to show that European TSOs have found interesting answers to problems envisaged during the early discussions of market coupling [Ehrenmann and Smeers 2005]. However, we have also found issues which cannot be cured by FBMC procedures:

- The base case constitutes a central development of the European TSOs. It enables TSOs/market clearing entities to take into account intra-zonal trade and is thereby generally able to shift the FBMC domain close to a welfare-optimal dispatch. The better the D-2 forecasts of TSOs become, the higher is the expected cost-effectiveness in the CWE electricity markets.
- One fundamental shortcoming of zonally organized markets remains to be the ex-ante determination of zonal PTDFs by use of GSKs, which makes load flow constraints inaccurate. In almost all cases with constrained exchange capacities, this entails welfare losses and/or redispatch. Researchers have proposed novel methods for GSK calculation (cf. [Voswinkel et al., 2019; Schönheit et al., 2020]). However, our analyses show how zonal PTDFs disregard nodal information and how these imperfections can impact market results and redispatch. Improved GSKs may change this to a limited extent, but the fundamental shortcoming will remain.
- Our results further call the cost-efficiency of the associated redispatch into question. In our 4-node example, a cost-efficient redispatch could only be attained coincidentally. In a realistic setting with thousands of nodes, increasing redispatch will deteriorate welfare.
- While the consideration of intra-zonal load flow constraints can prevent line overloads, we show that the effectiveness of managing congestion of intra-zonal lines in FBMC is inferior to nodal congestion management. Structurally overloaded intra-zonal lines lead to the dilemma of either having to restrict cross-zonal trade or to accept redispatch. Notably, this is nothing which could be cured by a change of FBMC procedures. Instead, this calls for price zone delimitations oriented towards the most congested lines.

While our analyses have revealed key benefits and weaknesses of FBMC as currently used in CWE, our analyses have some limitations:

- Notably, with a system containing few nodes, PTDFs are relatively high and PTDFs of the same line are very different for individual nodes within the same zone. Thus, loading of transmission lines is highly sensitive in our stylized model (cf. Fig. 4), and effects may consequently be overdrawn.
- The FBMC procedures in this paper are abstracted from the real-world processes to some extent. For instance, a base case without any net exports (as assumed in some parts of this study), is very unlikely to occur in practice. This leads to overdrawn effects of GSK inaccuracies. However, using a base case of all zeros is important for disaggregating the effects of FBMC elements and thereby illustrating the nature of inaccuracies that these elements entail.

• We have further neglected some aspects that are used in actual practice. For instance, the reference flows mentioned in section 2.2 are one example of these simplifications. Furthermore, we have not considered the N-1 criterion. In section 2.2.2, we have stated that the N-1 criterion would not fundamentally alter the results. Having illustrated the features of FBMC in the previous sections, we now comment more specifically on the N-1 criterion as follows. Of course, the consideration of the N-1 criterion will have a substantial effect on welfare in a zonal as well as in a nodal market design since the feasible region can only become smaller. However, the nature of the inaccuracies of FBMC will remain unchanged. I.e., line load sensitivities will be averaged due to the use of GSKs, the base case shifts and distorts the feasible region of the zonal EMCP around a point of reference, and the FRMs introduce a safety margin for inherent inaccuracies. These general conclusions remain unchanged with or without taking the N-1 criterion into account.

To some extent, all stylized models have these common characteristics that differ from the real world – even when not dealing with FBMC (cf. [Bjørndal and Jörnsten 2001; Bjørndal et al., 2003; Ehrenmann and Smeers 2005; Bjørndal and Jörnsten 2007; Oggioni and Smeers 2013; Grimm et al., 2016a, b]).

We note that our benchmark was chosen on a counterfactual basis. While the benchmark design, nodal pricing, is implemented in parts of the US and other regions of the world, it is not likely to be implemented in Europe any time soon. So this paper shows where the FBMC lacks

efficiency compared to a rather theoretical optimum (from a European point of view). However, it is necessary to show where efficiency is lost in order to be able to improve the procedures and concepts of FBMC.

For all of the above, our analyses have revealed how the FBMC elements affect the FBMC domain, ultimately resulting in welfare changes. These results provide comprehensive insights for policy-makers, regulators and TSOs, enabling them to sharpen the focus of large-scale assessments of electricity markets.

**Declaration of competing interest**

The authors declare that they have no known competing financial interests or personal relationships that could have appeared to influence the work reported in this paper.

**Acknowledgements**

This research has partly been funded by the Federal Ministry for Economic Affairs and Energy (BMWi) of Germany within the framework of the joint project “KoNeMaSim – Kopplung von Netz-und Markt-simulationen für die Netzplanung” (project number 03ET7526). The authors gratefully acknowledge the financial support. We further thank conference and workshop participants at ÖGOR Workshop Vienna, the 40th and 41st IAEE International Conferences as well as Steven Gabriel, Benjamin Hobbs and William Hogan for valuable comments.

**A. Generation and power flows for bases cases**

**Table 8**  
Generation and power flows for bases cases  $(e)_1$  and  $(e)_2$

		1	2	3	4
base case $(e)_1$	$q_i^{(e)}$	−136.4 MW	−82.1 MW	246.4 MW	27.9 MW
base case $(e)_2$	$q_i^{(e)}$	−105.6 MW	71.9 MW	−215.6 MW	249.4 MW
	$\alpha$	$\beta$	$\gamma$	$\delta$	$\epsilon$
base case $(e)_1$	−61.4 MW	−75 MW	−130 MW	−13.6 MW	116.4 MW
base case $(e)_2$	−30.6 MW	−75 MW	85.6 MW	−44.4 MW	−130 MW

**B. Abbreviations and symbols**

List of abbreviation	
(N)SFD	(non-)standard flow direction.
ATC	available transfer capacity.
CWE	Central Western Europe (=France, Belgium, Luxembourg, the Netherlands and Germany).
EMCP	electricity market clearing problem.
Entso-E	European Network of Transmission System Operators.
FAV	final adjustment value.
FBMC	flow-based market coupling.
FR	feasible region (as used here: the feasible region that is defined solely by the grid constraints of the EMCP).
FRM	flow reliability margin.
GSK	generation shift key.
LFC	load flow constraint.
NER	net export ratio.
PTDF	power transfer distribution factor.
RAM	remaining available margin.
TSO	transmission system operator.
List of symbols	
$A_{f,i}$	PTDF of line $f$ for net export at node $i$ .
$\bar{A}_{f,z}$	zonal PTDF of line $f$ for net export from zone $z$ .
$c_i(g_i)$	marginal costs of electricity generation at node $i$ (being a function of $g_i$ ).
$C_f$	capacity of line $f$ .
$d_i$	demand at node $i$ .
$\bar{d}_z$	aggregate demand in zone $z$ .
$(e)_{0/1}$	considered base cases.

(continued on next page)

(continued)

$f \in F_{(x/cb)}$	index/set of lines (if with subscript: $x$ = chosen subset, $cb$ = critical branches; otherwise: all transmission lines).
$g_i$	electricity generation at node $i$ .
$g_i^{max}$	(available) electrical generation capacity at node $i$ .
$i \in I_z$	index/set of nodes of the system (if with index $z$ : nodes within price zone $z$ ).
$M_f$	flow reliability margin of line $f$ .
$q_i^{(e/r)}$	net exports at node $i$ (if with superscripts: $(e)$ = expected at D-2 stage, $(r)$ = realized).
$\bar{q}_z^{(e/r)}$	net exports from zone $z$ (if with superscripts: $(e)$ = expected at D-2 stage, $(r)$ = realized).
$R_f^{(n)std}$	remaining available margin of line $f$ in (non-)standard flow direction.
$r_{z,i}^{abs.(e/r)}$	expected/realized net export ratio.
$V_f$	final adjustment value.
$z \in Z$	index/set of price zones.
$\Delta L_f^{(e)}$	expected line loading offset of line $f$ .
$\Delta t$	time step.
$\lambda_{z,i}^{inc.(p/r)}$	GSK of node $i$ in zone $z$ (superscripts: $(p)$ = predetermined at D-2 stage, $(r)$ = realized).

## References

- Amprion GmbH, 2014. Documentation of the CWE FB MC Solution as Basis for the Formal Approval-Request. [https://www.bundesnetzagentur.de/DE/Sachgebi.ete/ElektrizitaetundGas/Unternehmen\\_Institutionen/Netzzugang\\_Messwesen/Markt/opplung\\_Strom/Marktkopplung-node.html](https://www.bundesnetzagentur.de/DE/Sachgebi.ete/ElektrizitaetundGas/Unternehmen_Institutionen/Netzzugang_Messwesen/Markt/opplung_Strom/Marktkopplung-node.html). (Accessed 17 November 2019).
- Androce, I., Krajcar, S., 2012. Methodology of market coupling/splitting for efficient cross-border electricity trading. In: 2012 9th International Conference on the European Energy Market, pp. 1–8.
- Aravena Solis, I.A., 2019. Analysis of Renewable Energy Integration in Transmission-Constrained Electricity Markets Using Parallel Computing (PhD thesis. UC Louvain).
- Bjørndal, M., Jørnsten, K., Pignon, V., 2003. Congestion management in the nordic power market - counter purchase and zonal pricing. *J. Netw. Ind.* 4 (3), 271–291.
- Bjørndal, M., Jørnsten, K., 2001. Zonal pricing in a deregulated electricity market. *Energy J.* 51–73.
- Bjørndal, M., Jørnsten, K., 2007. Benefits from coordinating congestion management—the Nordic power market. In: *Energy Policy* 35.3, pp. 1978–1991.
- Dierstein, C., 2017. Impact of Generation Shift Key determination on flow based market coupling. In: 14th International Conference on the European Energy Market (EEM), Dresden.
- Ehrenmann, A., Smeers, Y., 2005. Inefficiencies in European congestion management proposals. In: *Utilities Policy* 13.2, pp. 135–152.
- Elia System Operator, S.A., 2017. Loop Flows Calculation. <http://www.elia.be/en/grid-data/interconnections/Loopflows>. (Accessed 17 November 2018).
- Elia System Operator, S.A., 2015. Implementation of day-ahead flow-based market coupling in the CWE region. Tech. rep.
- European Network of Transmission System Operators for Electricity (Entso-E), 2016. Entso-E Generation and Load Shift Key Implementation Guide. Brussels, Belgium. <https://docs.entsoe.eu/dataset/edi-generation-and-load-shift-key-imp-guide/re-source/1203dc88-8a10-48e6-93bc-8e782ce905b3>. (Accessed 17 November 2019).
- European Network of Transmission System Operators for Electricity (Entso-E), 2018. First Edition of the Bidding Zone Review - Draft Version for Public Consultation. <http://www.entsoe.eu/news/2018/04/05/first-edition-of-the-bidding-zone-review-published/>. (Accessed 17 November 2019).
- Finck, R., Ardone, A., Fichtner, W., 2018. Impact of flow-based market coupling on generator dispatch in CEE region. In: 2018 15th International Conference on the European Energy Market (EEM). IEEE, Piscataway, New Jersey, pp. 1–5.
- Grimm, V., Martin, A., Weibelzahl, M., Zöttl, G., 2016a. On the long run effects of market splitting: why more price zones might decrease welfare. In: *Energy Policy*, vol. 94, pp. 453–467.
- Grimm, V., et al., 2016b. Transmission and generation investment in electricity markets: the effects of market splitting and network fee regimes. In: *European Journal of Operational Research* 254.2, pp. 493–509.
- Jegleim, B., 2015. Flow Based Market Coupling. Master thesis. <http://hdl.handle.net/11250/2368078>. visited on 11/07/2018.
- Kristiansen, T., 2020. The flow based market coupling arrangement in Europe: implications for traders. In: *Energy Strategy Reviews*, vol. 27, p. 100444. <http://www.sciencedirect.com/science/article/pii/S2211467X19301373>.
- Lang, L.M., Dallinger, B., Lettner, G., 2020. The meaning of flow-based market coupling on redispatch measures in Austria. In: *Energy Policy*, vol. 136, p. 111061. <http://www.sciencedirect.com/science/article/pii/S0301421519306482>.
- Marjanovic, I., Stein, v., D, van Bracht, N., Moser, A., 2018. Impact of an enlargement of the flow based region in continental Europe. In: 2018 15th International Conference on the European Energy Market (EEM), pp. 1–5.
- Matthes, B., Spieker, C., Klein, D., Rehtanz, C., 2019. Impact of a minimum remaining available margin adjustment in flow-based market coupling. In: 2019 IEEE Milan PowerTech, pp. 1–6.
- Morin, T., 2016. Statistical Study and Clustering of the Critical Branches Defining the Market Coupling in the Central West Europe Zone. Master thesis. <http://www.diva-portal.org/smash/record.jsf?pid=diva2%3A930849&dsid=-5954>. (Accessed 11 July 2018).
- Neuhoff, K., et al., 2013. Renewable electric energy integration: quantifying the value of design of markets for international transmission capacity. In: *Energy Economics*, vol. 40, pp. 760–772.
- Oggioni, G., Smeers, Y., 2012. Degrees of coordination in market coupling and counter-trading. In: *The Energy Journal* 33.3, pp. 39–90.
- Oggioni, G., Smeers, Y., 2013. Market failures of Market Coupling and counter-trading in Europe: an illustrative model based discussion. In: *Energy Economics*, vol. 35, pp. 74–87.
- Plancke, G., et al., 2016. Efficient use of transmission capacity for cross-border trading: available Transfer Capacity versus flow-based approach. In: 2016 IEEE International Energy Conference (ENERGYCON), pp. 1–5.
- Réseau de transport d'électricité (RTE), 2015. CWE Flow Based Market-Coupling Project: Parallel Run Performance Report. (Accessed 17 November 2019). [http://www.jao.eu/support/reso\\_urcecenter/overview?parameters=%7B%22isCWEFBMCRelevantDocumentation%22%3A%22True%22%7D](http://www.jao.eu/support/reso_urcecenter/overview?parameters=%7B%22isCWEFBMCRelevantDocumentation%22%3A%22True%22%7D).
- Schönheit, D., Sikora, R., 2018. A statistical approach to generation shift keys. In: 2018 15th International Conference on the European Energy Market (EEM), pp. 1–6.
- Schönheit, D., Weinhold, R., Dierstein, C., 2020. The impact of different strategies for generation shift keys (GSKs) on the flow-based market coupling domain: a modelbased analysis of Central Western Europe. In: *Applied Energy*, vol. 258, p. 114067. <http://www.sciencedirect.com/science/article/pii/S0306261919317544>.
- Sebestyén, M., Divenyi, D., Sörös, P., 2018. An enhanced calculation method of generation shift keys in flow based market coupling. In: 2018 15th International Conference on the European Energy Market (EEM), pp. 1–5.
- Van den Bergh, K., Boury, J., Delarue, E., 2016. The flow-based market coupling in central western Europe: concepts and definitions. In: *The Electricity Journal* 29.1, pp. 24–29.
- Voswinkel, S., Felten, B., Felling, T., Weber, C., 2019. What Drives Welfare in Europe's Approach to Electricity Market Coupling? HEMF Working Paper No. 08/2019. House of Energy Markets and Finance. <https://ssrn.com/abstract=3424708>.
- Wyrwoll, L., Blank, A., Müller, C., Puffer, R., 2019. Determination of preloading of transmission lines for flow-based market coupling. In: 2019 16th International Conference on the European Energy Market (EEM), pp. 1–6.
- Wyrwoll, L., Kollenda, K., Müller, C., Schnettler, A., 2018. Impact of flow-based market coupling parameters on European electricity markets. In: 2018 53rd International Universities Power Engineering Conference (UPEC), pp. 1–6.
- Xie, J., Hong, T., 2016. GEFCom2014 probabilistic electric load forecasting: an integrated solution with forecast combination and residual simulation. In: *International Journal of Forecasting* 32.3, pp. 1012–1016.
- Ziel, F., Liu, B., 2016. Lasso estimation for GEFCom2014 probabilistic electric load forecasting. In: *International Journal of Forecasting* 32.3, pp. 1029–1037.
- Zimmermann, R., Murillo-Sánchez, C., Thomas, R., 2011. MATPOWER: steady-state operations, planning and analysis tools for power system research and education. In: *IEEE Transactions on Power Systems* 26.1, pp. 12–19.

# DuEPublico

Duisburg-Essen Publications online

UNIVERSITÄT  
DUISBURG  
ESSEN

*Offen im Denken*

ub

universitäts  
bibliothek

This text is made available via DuEPublico, the institutional repository of the University of Duisburg-Essen. This version may eventually differ from another version distributed by a commercial publisher.

**DOI:** 10.1016/j.jup.2020.101136

**URN:** urn:nbn:de:hbz:465-20250103-105455-1



This work may be used under a Creative Commons Attribution 4.0 License (CC BY 4.0).